Microscopic analysis of shape transition in neutron-deficient Yb isotopes

Y. Fu,[1,*] H. Tong,[1] X. F. Wang,[1] H. Wang,[1] D. Q. Wang,[1] X. Y. Wang,[2] and J. M. Yao[3,†]
[1]*School of Mechatronics Engineering, Guizhou Minzu University, Guiyang 550001, China*
[2]*School of Electrical Engineering, Xuchang University, Xuchang 461000, China*
[3]*Department of Physics and Astronomy, University of North Carolina, Chapel Hill, North Carolina 27516-3255, USA*

(Received 2 September 2017; revised manuscript received 30 October 2017; published 22 January 2018)

The development of nuclear collectivity in even-even $^{152-170}$Yb is studied with three types of mean-field calculations: the nonrelativistic Hartree-Fock plus BCS calculation using the Skyrme SLy4 force plus a density-dependent δ pairing force and the relativistic mean-field calculation using a point-coupling energy functional supplemented with either a density-independent δ pairing force or a separable pairing force. The low-lying states are obtained by solving a five-dimensional collective Hamiltonian with parameters determined from the three mean-field solutions. The energy surfaces, excitation energies, electric multiple transition strengths, and differential isotope shifts are presented in comparison with available data. Our results show that different treatments of pairing correlations have a significant influence on the speed of developing collectivity as the increase of neutron number. All the calculations demonstrate the important role of dynamic shape-mixing effects in resolving the puzzle in the dramatic increase of charge radius from ^{152}Yb to ^{154}Yb and the role of triaxiality in ^{160,162,164}Yb.

DOI: 10.1103/PhysRevC.97.014311

I. INTRODUCTION

The collectivity or equilibrium shape of atomic nucleus and its evolution with respect to nucleon number have been an intensively studied subject in nuclear physics. They provide rich information about the interplay of nuclear collectivity and underlying shell structure. This information can be learnt from the changes in both nuclear bulky properties and the spectroscopic properties of low-lying states. The nuclei with proton number $Z \approx 70$–80 and neutron number N in between the two magic numbers 82 and 126 have attracted lots of research interests. These nuclei generally exhibit a transition from the spherical or weakly deformed shape to a well-deformed prolate shape and then back to a weakly oblate shape. At some point of the shape evolution, multiple shapes coexist at low energy and enrich the structure of their low-lying states. Besides the availability of rich experimental data on the low-lying states of these nuclei, a large number of theoretical studies have also been carried out. See, for instance, the microscopic studies based on energy density functional (EDF) methods [1–7].

In this work, we are focusing on the development of collectivity in neutron-deficient Yb isotopes, which has not been comprehensively studied. Experimentally, Sprouse *et al.* measured the isotope shifts of even-even $^{152-158,166}$Yb isotopes and they found that the rms charge radius at $N = 84$ is surprisingly larger than that at $N = 82$, which is quite exceptional in the nucleus of this mass region [8]. An assumption of strong deformation jump at ^{154}Yb was made to explain this strange behavior. However, this assumption was not supported by the latter measurements on the isotope shift and hyperfine structure for the adjacent odd isotopes ^{153,155}Yb [9]. The small difference between the rms radii of ^{154}Yb and ^{155}Yb, together with the small quadrupole moment of the ^{155}Yb, indicates that the deformation of ^{154}Yb should be small as well. The fast rise of the rms radius from $N = 82$ to $N = 84$ for Yb isotopes becomes a puzzle, the understanding of which requires more experiments. Recently, the calculation with the total Routhian surface method has shown that the ground state of ^{155}Yb exhibits a triaxial shape and the low-lying states are soft in quadrupole shapes [10]. Moreover, the structural characters observed in ^{157}Yb provide some hints for coexistence of three distinct shapes: prolate, triaxial, and oblate. All of these facts motivate us to carry out a systematic investigation of the low-lying states in neutron-deficient Yb isotopes to understand their evolution behaviors.

The nuclear EDF methods are the only ones that can presently be used for nuclei throughout the chart. Modern EDFs provide the most complete and accurate description of structure phenomena related to the evolution of nuclear shape and shell structure in medium-mass and heavy nuclei. To describe nuclear spectroscopy of low-lying states, one should go beyond the mean-field approximation to take into account the restorations of broken symmetries and/or the configuration mixing of intrinsic states in the framework of generator coordinate method (GCM). In the past decades, the GCM combined with the exact projection techniques has been implemented into the modern EDF calculations [11–17]. In this kind of study, calculations may become computationally demanding and time-consuming, particularly when the triaxiality degree of freedom is included in the analysis. Up to now, such kind of study has been mostly restricted to light nuclei [14,18,19] and some specific medium-heavy nuclei [20–23].

*fuyungzmd@163.com
†Corresponding author: yao.jiangming@gmail.com

As Gaussian overlap approximation of the exact GCM, a five-dimensional collective Hamiltonian (5DCH) with quadrupole degrees of freedom is alternatively adopted for the description of nuclear low-lying collective states. The vibrational mass parameters, rotational moments of inertia, and the collective potential are determined from the self-consistent mean-field calculations with a given EDF. This 5DCH method is much simpler in numerical calculations than the exact GCM calculation, and has achieved great success in description of nuclear low-lying states in a wide range of nuclei, from the mass number $A \sim 40$ to superheavy regions including the spherical, transitional, and deformed nuclei [24–33]. In particular, the validity of the 5DCH method has been demonstrated by comparing with the seven-dimensional GCM calculation for ^{76}Kr based on a relativistic EDF [22]. In this paper, we adopt the 5DCH for the low-lying states of Yb isotopes with the collective parameters determined by the mean-field solutions of both a non-relativistic Skyrme EDF and a relativistic point-coupling EDF. Pair correlations are treated in the Bardeen-Cooper-Schrieffer (BCS) method using either a δ force or a separable force.

The paper is organized as follows. In Sec. II, we will introduce briefly our method used to study the low-lying states in neutron-deficient Yb isotopes. The results and discussions will be presented in Sec. III. A summary is made in Sec. IV.

II. THE ENERGY-FUNCTIONAL-BASED COLLECTIVE HAMILTONIAN METHOD

The collective excitations of a quadrupole deformed nucleus can be mainly classified into rotational and vibrational motions. Considering the energy scales of these two motions are not well separated in atomic nuclei, the coupling between these two motions is expected to be important. Therefore, the 5DCH that describes the collective excitations of a quadrupole deformed nucleus can be written in the form [34]

$$\hat{H} = \hat{T}_{\rm vib} + \hat{T}_{\rm rot} + V_{\rm coll}. \tag{1}$$

The kinetic terms for the vibrational and rotational motions have the standard form

$$\hat{T}_{\rm vib} = \frac{1}{2} B_{\beta\beta}\dot{\beta}^2 + \beta B_{\beta\gamma}\dot{\beta}\dot{\gamma} + \frac{1}{2}\beta^2 B_{\gamma\gamma}\dot{\gamma}^2, \tag{2}$$

$$\hat{T}_{\rm rot} = \frac{1}{2}\sum_{k=1}^{3} \mathcal{I}_k \omega_k^2, \tag{3}$$

where ω_k is the rotational frequency. The mass parameters $B_{\beta\beta}$, $B_{\beta\gamma}$, $B_{\gamma\gamma}$, as well as the moments of inertia $\mathcal{I}_k$, depend on the Bohr parameters (β,γ),

$$\mathcal{I}_k = 4B_k\beta^2 \sin^2(\gamma - 2k\pi/3), \quad k = 1,2,3. \tag{4}$$

After quantization, one finds the kinetic terms as

$$\begin{aligned}\hat{T}_{\rm vib} = -\frac{\hbar^2}{2\sqrt{wr}}\Bigg\{ &\frac{1}{\beta^4}\Bigg[\frac{\partial}{\partial\beta}\sqrt{\frac{r}{w}}\beta^4 B_{\gamma\gamma}\frac{\partial}{\partial\beta} \\ &-\frac{\partial}{\partial\beta}\sqrt{\frac{r}{w}}\beta^3 B_{\beta\gamma}\frac{\partial}{\partial\gamma}\Bigg] + \frac{1}{\beta\sin 3\gamma}\Bigg[-\frac{\partial}{\partial\gamma}\sqrt{\frac{r}{w}}\sin 3\gamma \\ &\times B_{\beta\gamma}\frac{\partial}{\partial\beta} + \frac{1}{\beta}\frac{\partial}{\partial\gamma}\sqrt{\frac{r}{w}}\sin 3\gamma\, B_{\beta\beta}\frac{\partial}{\partial\gamma}\Bigg]\Bigg\},\end{aligned} \tag{5}$$

and

$$\hat{T}_{\rm rot} = \frac{1}{2}\sum_{k=1}^{3}\frac{\hat{J}_k^2}{\mathcal{I}_k}, \tag{6}$$

with $\hat{J}_k$ denoting the components of the angular momentum in the body-fixed frame of a nucleus. The quantities $r = B_1B_2B_3$ and $w = B_{\beta\beta}B_{\gamma\gamma} - B_{\beta\gamma}^2$ determine the volume element in the collective space.

In the EDF-based collective Hamiltonian calculations [24,25,27], the potential $V_{\rm coll}$ is determined in the following way:

$$V_{\rm coll}(\beta,\gamma) = E_{\rm tot}(\beta,\gamma) - \Delta V_{\rm vib}(\beta,\gamma) - \Delta V_{\rm rot}(\beta,\gamma), \tag{7}$$

with $E_{\rm tot}(\beta,\gamma)$ being the energy of the mean-field state. The $\Delta V_{\rm vib}$ and $\Delta V_{\rm rot}$ are zero-point energy of vibrational and rotational motions respectively.

The dynamics of the 5DCH is governed by the seven functions of the intrinsic deformations β and γ: the collective potential $V_{\rm coll}$, the three mass parameters ($B_{\beta\beta}$, $B_{\beta\gamma}$, $B_{\gamma\gamma}$), and the three moments of inertia $\mathcal{I}_k$. In principle, one should calculate the inertia parameters using the formulas derived from the GCM method, which correspond to the Peiers-Yoccoz inertia [34]. As discussed in Ref. [22], however, the Hill-Wheeler integral in the conventional GCM method runs over only the collective coordinates without the corresponding momenta. Therefore, it is generally assumed that one should use the Thouless-Valatin inertia parameters [35], which can be alteratively determined by the normal modes of local quasi-particle random-phase approximation [36]. The determination of inertia parameters in this way based on the solutions of energy density functional methods is very complicated. To simplify the calculation, one usually adopts the Inglis-Belyaev formula for the rotational inertia and a similar expression for the inertia in the vibrational degrees of freedom [26,27,37]. It is known that the cranking formulas without the contribution from time-odd components in the mean field generally result in a stretched energy spectrum by a factor of 1.2–1.4.

III. RESULTS AND DISCUSSION

The Dirac equation for single-nucleon wave functions in relativistic mean-field (RMF) approach is solved in the basis of eigenfunctions of a three-dimensional harmonic oscillator in Cartesian coordinate with 14 major shells, which are found to be sufficient to obtain a reasonably converged results for the nuclei of this mass region. The oscillator frequency is given by $\hbar\omega_0 = 41A^{-1/3}$ (MeV), where A is the mass number. The like-particle pairing correlations between nucleons are treated

using either a density-independent δ force (DIDF)

$$V_\tau(\mathbf{r}_1,\mathbf{r}_2,\mathbf{r}_1',\mathbf{r}_2') = V_\tau^{pp}\delta(\mathbf{r}_1-\mathbf{r}_1')\delta(\mathbf{r}_1-\mathbf{r}_2)\delta(\mathbf{r}_2-\mathbf{r}_2'), \quad (8)$$

supplemented with a smooth energy-dependent cutoff or using the separable pairing force proposed by Tian, Ma, and Ring (TMR) [39]

$$V_\tau(\mathbf{r}_1,\mathbf{r}_2,\mathbf{r}_1',\mathbf{r}_2') = -G\delta(\mathbf{R}-\mathbf{R}')\frac{1}{(4\pi a^2)^3}e^{-(r^2+r'^2)/4a^2}, \quad (9)$$

where $\mathbf{R} = (\mathbf{r}_1+\mathbf{r}_2)/2$ and $\mathbf{r} = \mathbf{r}_1-\mathbf{r}_2$. The strengths V_τ^{pp} in the DIDF pairing force -349.5 MeV fm^3 and -330.0 MeV fm^3 for neutrons and protons, respectively, were determined by fitting to the pairing gaps of some finite nuclei globally [38]. The parameters in the TMR separable pairing force $G = -728$ MeV fm^3 and $a = 0.644$ fm were determined by fitting to the pairing gap of Gogny force D1S for nuclear matter [39].

For the mean-field calculation with the nonrelativistic Skyrme SLy4 [40] force, we adopted the computer code EV8 [41], in which the Hartree-Fock (HF) plus BCS equations are solved by discretizing individual single-particle wave functions on a three-dimensional Cartesian mesh. The like-particle pairing correlations are taken into account with a density-dependent δ force (DDDF),

$$V_\tau(\mathbf{r}_1,\mathbf{r}_2,\mathbf{r}_1',\mathbf{r}_2') = V_\tau^{pp}\left[1-\frac{\rho(\mathbf{r})}{\rho_0}\right]\delta(\mathbf{r}_1-\mathbf{r}_1')\delta(\mathbf{r}_1-\mathbf{r}_2)\delta(\mathbf{r}_2-\mathbf{r}_2'), \quad (10)$$

with the parameters $V_\tau^{pp} = -1000$ MeV fm^3 and $\rho_0 = 0.16$ fm^{-3} for both neutrons and protons and with a soft cutoff at 5 MeV above and below the Fermi energy. More details can be found in Ref. [41].

In both calculations, a set of intrinsic triaxially deformed states with $\beta \in [0.0,0.6]$ and $\gamma \in [0°,60°]$, step size $\Delta\beta = 0.1$ and $\Delta\gamma = 10°$ is adopted to determine the parameters in the collective Hamiltonian. The Bohr deformation parameters (β,γ) are defined through the quantities q_{20} and q_{22},

$$\beta = \frac{4\pi}{3AR_0^2}\sqrt{q_{20}^2+2q_{22}^2}, \quad \gamma = \tan^{-1}\left(\sqrt{2}\frac{q_{22}}{q_{20}}\right) \quad (11)$$

with $q_{2\mu} = \langle r^2 Y_{2\mu}\rangle$ and $R_0 = 1.2A^{1/3}$ fm. The 5DCH is solved in a set of basis functions that depend on the deformation variables β and γ, and three Euler angles [42].

Figures 1 and 2 display the potential energy surfaces of $^{152-158}$Yb isotopes in the β-γ plane from the RMF+BCS and Skyrme HF+BCS calculations, respectively. In both cases, the shift of the global minimum in the energy surface exhibits a picture of shape transition from a spherical vibrator to a prolate deformed rotor when the neutron number increases from $N = 82$ to $N = 100$. Similar to the cases for Sr and Zr isotopes around $N = 60$ [29], however, the SLy4 force presents more rapid development of collectivity, in comparison with that by the PC-PK1 force. In particular, one finds that the deformation energy surfaces by the SLy4 force are much stiffer around the global minimum and exhibit more complicated structures in most of the isotopes. The potential energy surfaces of ^{156}Yb and ^{158}Yb show that their oblate and prolate energy minima are connected with triaxiality degree of freedom. Whether there is a coexistence of prolate, triaxial, and oblate shapes at close

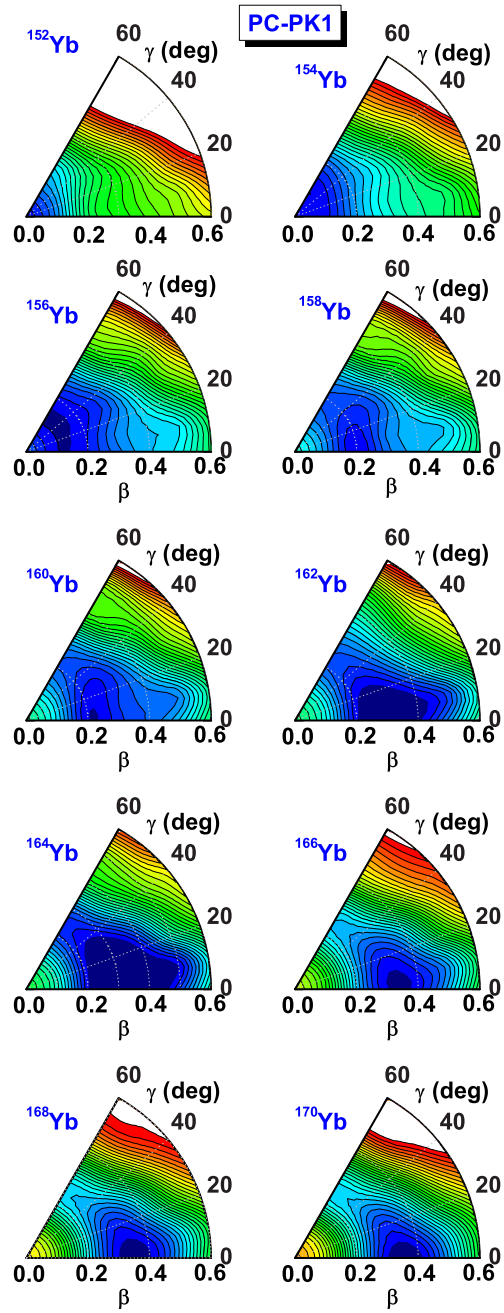

FIG. 1. Mean-field energy $E_{\rm tot}$ of $^{152-170}$Yb isotopes in the β-γ plane, from the constrained RMF + BCS calculations with the PC-PK1 parametrization for the particle-hole (ph) channel and density-independent δ force (DIDF) for the particle-particle (pp) channel. All energies are normalized to the absolute minimum. Each contour line is separated by 0.5 MeV.

energy in low-lying states of these two nuclei or not requires beyond mean-field calculations.

The energy minimum of ^{154}Yb from the mean-field calculations using either the PC-PK1 (DIDF) or the PC-PK1 (TMR) is located at a weakly deformed oblate shape with $\beta = 0.1$ and $\gamma = 60°$. The difference in the squared charge radii of the energy-minimum states in ^{152}Yb and ^{154}Yb is predicted to be about 0.30 fm^2 in both calculations. This value is much

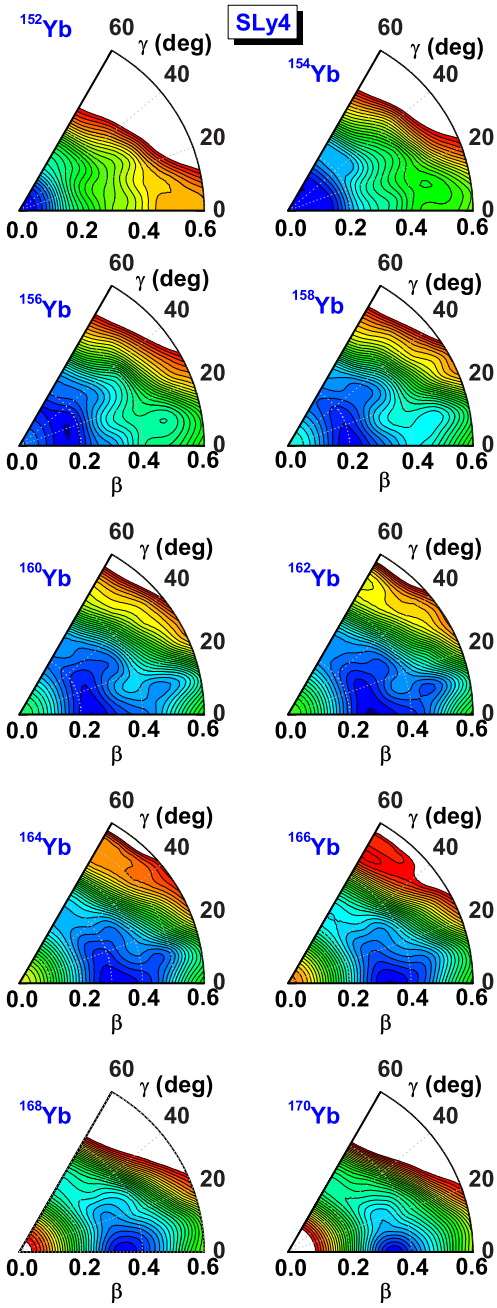

FIG. 2. Same as Fig. 1, but by the SLy4 force for the ph channel and density-dependent δ force (DDDF) for the pp channel.

smaller than the data, 0.49 fm^2. It indicates that the mean-field calculation is not sufficient to reproduce the dramatic increase in the rms charge radius from ^{152}Yb to ^{154}Yb.

Figure 3 displays the systematics of excitation energies and electric quadrupole ($E2$) transition strengthes of the low-lying states in neutron-deficient Yb isotopes, in comparison with the data [43]. As the neutron number goes away from the magic number $N = 82$, the yrast states fall down smoothly and become members of the prolate deformed rotation band. The systematics in both excitation energies and quadrupole transition strengths are reproduced reasonably by our calculations. Quantitatively, the $E2$ transition strengths are over-

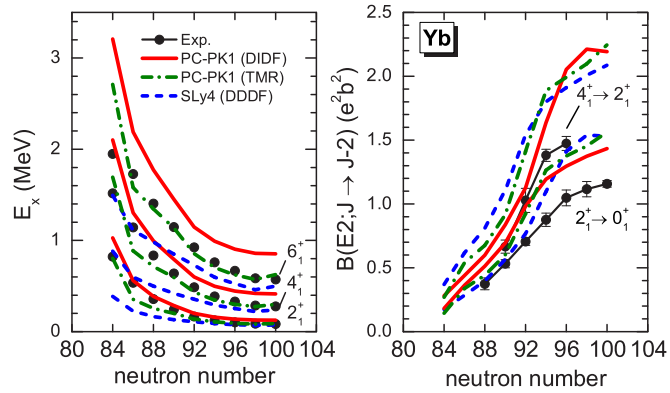

FIG. 3. Systematics of excitation energies and electric quadrupole transition strengths for the ground-state rotational band in neutron-deficient Yb isotopes, in comparison with the data [43].

all overestimated by $\sim 33\%$. Comparing the predictions by different types of calculations with the data, one finds the PC-PK1 (DIDF) underestimates the moment of inertia, while the SLy4 (DDDF) overestimates it. The PC-PK1 (TMR) with the separable pairing force predicts the excitation energies in between and closest to the data. It is shown in Fig. 4 that the average pairing gap $\langle\Delta\rangle^{uv}$ by the PC-PK1 (DIDF) is overall larger than that by the PC-PK1 (TMR). The $\langle\Delta\rangle^{uv}$ is defined as

$$\langle\Delta\rangle^{uv} = \frac{\sum_k f_k u_k v_k \Delta_k}{\sum_k f_k u_k v_k}, \tag{12}$$

where v_k^2 and Δ_k are the occupation probability and pairing gap of the kth single-particle state, respectively, and $u_k^2 + v_k^2 = 1$. The f_k is an energy-dependent smooth cutoff [15]. As a result of the different treatment of pairing correlation, the moment of inertia by the former is overall smaller than that by the latter. Therefore, the energy spectrum by the PC-PK1 (DIDF) is

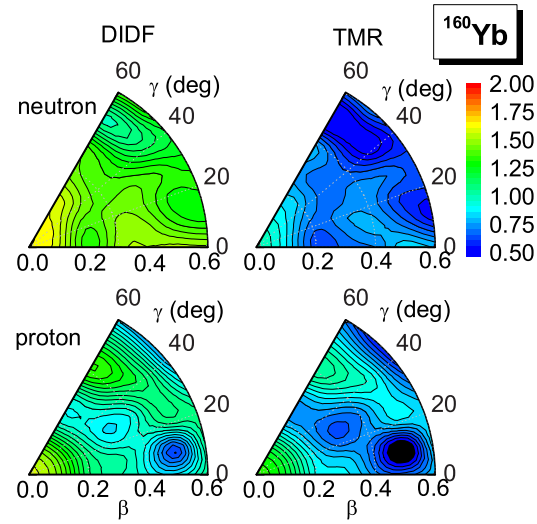

FIG. 4. Average pairing gaps $\langle\Delta\rangle^{uv}$ (in MeV) for neutrons and protons in ^{160}Yb from the RMF calculations with either the DIDF or the TMR force [39] for the pp channel.

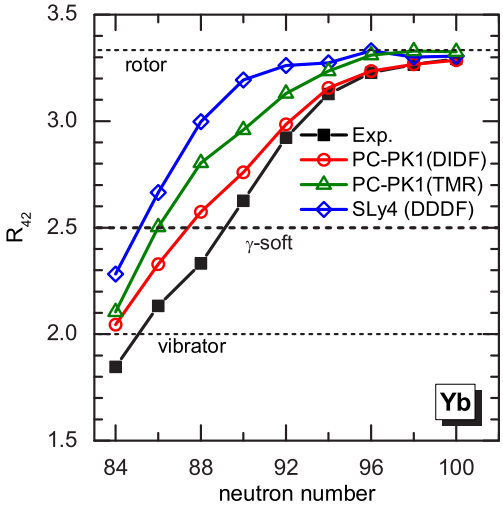

FIG. 5. The ratio $R_{42} = E_x(4^+_1)/E_x(2^+_1)$ as a function of neutron number in Yb isotopes from the 5DCH calculations with different forces, in comparison with the data [43].

more stretched than that by the PC-PK1 (TMR), as the stronger pairing tends to give the smaller moments of inertia.

Figure 5 displays the ratio $R_{42} = E_x(4^+_1)/E_x(2^+_1)$ as a function of neutron number in the Yb isotopes. The ratio R_{42} is often used to characterize nuclear shape transition between an axially deformed rotor ($R_{42} = 3.33$) and a spherical vibrational nucleus ($R_{42} = 2.00$). We note that all the calculations exhibit a picture of spherical-prolate shape transition when the neutron number increases from the magic number $N = 82$. However, the shape transition by the SLy4 force is too rapid, four neutrons earlier than the data. Moreover, the ratio R_{42} by the PC-PK1 (TMR) [39] exhibits a faster spherical to prolate shape transition than that by the PC-PK1 (DIDF). It indicates that a stronger pairing correlation between nucleons is necessary to reproduce the more moderate development of collectivity in the Yb isotopes.

Figure 6 shows the evolution of the excitation energies for the states (2^+_2,3^+_1,4^+_2,5^+_1,6^+_2) in the γ band. One can see that the excitation energy of the bandhead 2^+_2 state globally decreases as the neutron number increases from 82 to 90 or 94, which depends on the details of the calculations, and then increases again as the neutron number increases further. It can be understood from Figs. 1 and 2 that the energy surfaces are very soft along both β and γ directions around the energy minima in ^{160,162,164}Yb. As a result, the excitation energy of the bandhead (0^+_2) state also reaches the lowest value in these nuclei among the neutron-deficient Yb isotopes, as illustrated in Fig. 7. This is consistent with the evolution trend observed from the available data, even though they are very limited and the evolution is much more moderate. The excitation energy of the 0^+_2 state by the PC-PK1 (DIDF) in ^{162}Yb is $E_x = 0.894$ MeV, compared with the data $E_x = 1.006$ MeV. For ^{164}Yb, this value is $E_x = 1.027$ MeV, compared with the data $E_x = 0.976$ MeV.

Electric monopole ($E0$) transition strength is frequently adopted in the study of shape mixing in atomic nuclei. Generally speaking, the lower excitation energy of 0^+_2 state is

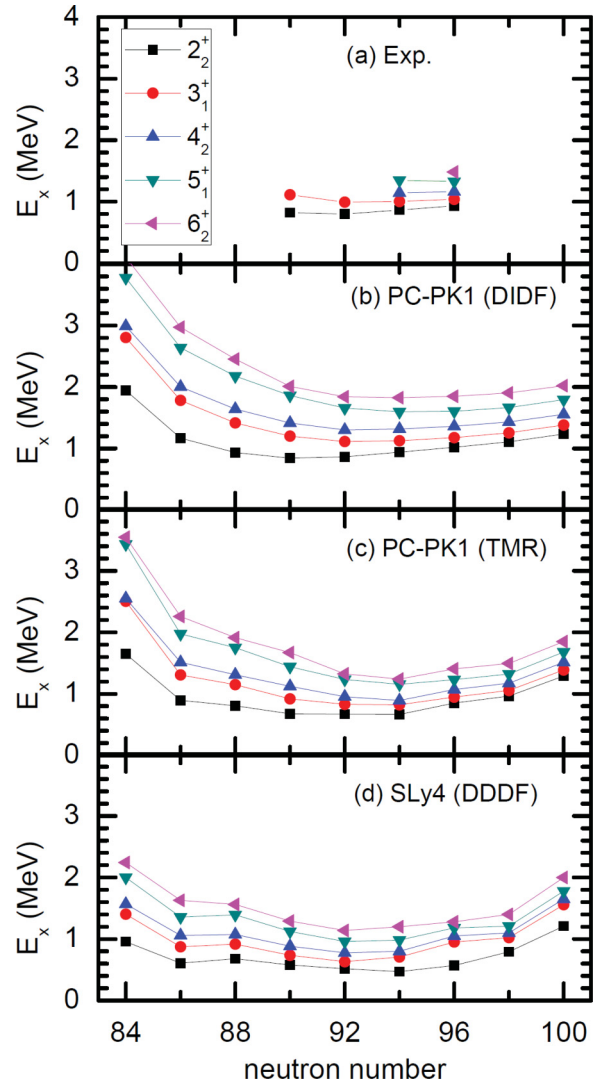

FIG. 6. Systematics of excitation energies for the states in the γ-band for the neutron-deficient Yb isotopes, in comparison with the data [43].

observed at the isotope with a larger ρ^2_{E0} value. Figure 7(a) shows that the electric monopole ($E0$) transition strength, which is defined as

$$\rho^2_{E0} = \left| \frac{\langle 0^+_2 | er^2 | 0^+_1 \rangle}{eR^2} \right|^2, \tag{13}$$

reaches to the minimal value in ^{92,94}Yb. According to Ref. [44], the $E0$ transition strength is correlated to the size of the deformation and to the amount of mixing between configurations corresponding to different shapes. Therefore, it provides an indicator of shape mixing. The predicted largest $E0$ strengths in ^{92,94}Yb indicate the strongest mixing between different shapes in these nuclei among the neutron-deficient Yb isotopes.

The evolution of the isotope shifts $\delta\langle r^2\rangle_{N,82}$ with respect to ^{152}Yb and the differential isotope shifts $\delta\langle r^2\rangle_{N,N-2} = \delta\langle r^2\rangle_N - \delta\langle r^2\rangle_{N-2}$ as a function of neutron number N is shown in Fig. 8. It is seen that the $\delta\langle r^2\rangle_{N,82}$ increases almost linearly

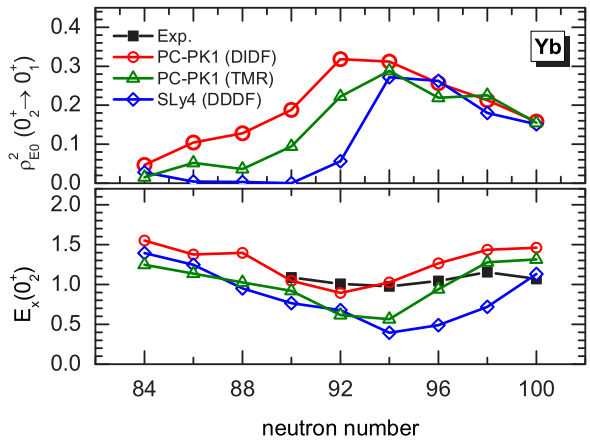

FIG. 7. Electric monopole transition strength $\rho^2_{E0}(0^+_2 \to 0^+_1)$ and excitation energy of 0^+_2 state as functions of neutron number in Yb isotopes from the 5DCH calculations with the PC-PK1 parametrization of covariant energy density functional, in comparison with the data [43].

with the neutron number, but with a kink at $N = 94$ in the results by the PC-PK1. This kink is shown more clearly in the plot for the differential isotope shifts, which exhibits a peak around $N = 92$ or 94. This behavior is consistent with the evolution of the predominate shape in the ground state of the Yb isotopes. The predicted value for the $\delta\langle r^2\rangle_{84,82}$ is 0.42, 0.35, and 0.33 fm^2 by the 5DCH calculations using the PC-PK1 (DIDF), PC-PK1 (TMR), and SLy4 (DDDF), respectively. Compared with the mean-field value ∼0.30 fm^2, the results by the 5DCH calculations are in better agreement with the data. In other words, the dynamic shape mixing effects are important to resolve the puzzle in the rapid increase of charge radii from ^{152}Yb to ^{154}Yb.

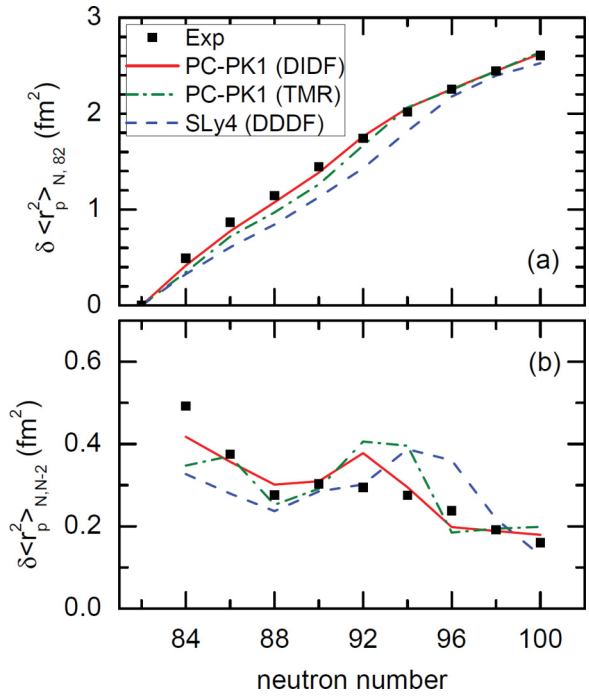

FIG. 8. Variation of the isotope shifts with respect to ^{152}Yb (upper panel) and the differential isotope shifts (lower panel) $\delta\langle r^2\rangle_{N,N-2} = \langle r^2\rangle_N - \langle r^2\rangle_{N-2}$ as a function of neutron number for the ground states of Yb isotopes, in comparison with the data [45].

The low-lying states of odd-mass Yb isotopes are challenges for the collective Hamiltonian as the treatment of Pauli-exclusion effect between the unpaired nucleon and the core nucleons is difficult, even though there is an attempt with the idea of core-quasiparticle coupling [46]. To shed light on the shape coexistence in ^{157}Yb, we study in detail the low-lying states of ^{156,158}Yb instead. A nucleus with "shape coexistence" is usually characterized with the presence of states at similar energy but possessing distinctly different intrinsic shapes. Figure 9 displays the low-lying energy spectra and the $E2$ transition strengths of ^{156,158}Yb from the 5DCH calculation with the PC-PK1 (DIDF). It is shown that the low-energy structures of ^{156,158}Yb are similar. For ^{156}Yb, the second 0^+ and 2^+ states and the first 4^+ state are almost degenerate. The whole energy spectrum exhibits the character of a quadrupole vibrator. We note that the reduced $E2$ transition matrix element in the ground-state band is not much different from that for the series of the states 0^+,2^+,4^+,6^+ on the left column. The $B(E2 : 4^+_1 \to 2^+_1)$ for ^{156}Yb is 0.62 e^{2}b^2, slightly smaller than the twice of the $B(E2 : 2^+_1 \to 0^+_1) = 0.36$ e^{2}b^2. This phenomenon is similar to the findings in ^{58}Ni [47] that the values of $B(E2 : 0^+_2 \to 2^+_1) = 0.27$ e^{2}b^2 and $B(E2 : 2^+_2 \to 2^+_1) = 0.50$ e^{2}b^2 are much smaller than what would be expected for a harmonic vibrator. In other words, there are larger anharmonicity effects in the $E2$ transition strengths than those in excitation energies. All these features indicate that the low-energy structure of ^{156}Yb is dominated by quadrupole vibration collective motions with a large anharmonicity, instead of shape coexistence. For ^{158}Yb, the β band is shifted upward and the $E2$ transition strengths are somewhat stronger, compared to ^{156}Yb. In other words, from ^{156}Yb to ^{158}Yb, the low-energy structure is changing from a quadrupole vibrator toward a prolate deformed rotor, accompanying triaxial γ softness. These findings are consistent with the potential energy surfaces shown in Fig. 1. It is worth mentioning that parity-doublet states have been observed experimentally in both ^{156}Yb and ^{158}Yb, the description of which requires the mixing of reflection-asymmetric intrinsic states in the calculations [48].

IV. SUMMARY

In this paper, we have studied in detail the evolution of low-lying collective states in the even-even $^{152-170}$Yb with the EDF based 5DCH, the parameters of which are determined with three types of mean-field calculations. The energy surfaces, excitation energies, electric multiple transition strengths, and differential isotope shifts have been analyzed in comparison with available data. The results exhibit a picture of spherical-prolate shape transition when the neutron number goes away from magic number $N = 82$. All the calculations exhibit a picture of spherical-prolate shape transition when the neutron number increases from the magic number $N = 82$. The results

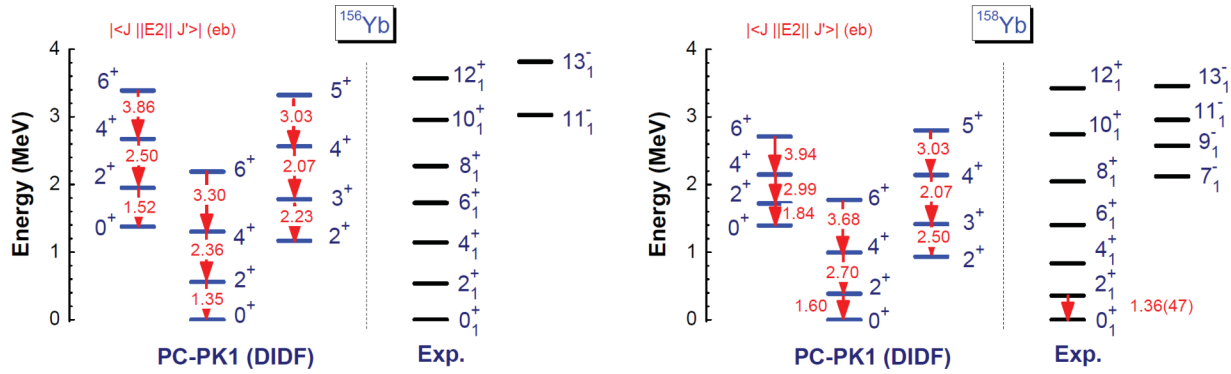

FIG. 9. Low-lying energy spectra of ^{156,158}Yb by the 5DCH calculation with the PC-PK1 (DIDF), in comparison with available data. The absolute value of the reduced transition matrix element $\langle J||E2||J'\rangle$ (in eb) is indicated on the arrows.

show that the calculation based on the SLy4 (DDDF) force predicts the most rapid spherical to prolate shape transition, while the PC-PK1 (DIDF) with the strongest pairing correlation gives the most moderate transition. In other words, different treatments of pairing correlations have a significant influence on the speed of developing collectivity as the increase of neutron number in the neutron-deficient Yb isotopes. The results from the three calculations have shown the important role of dynamic shape-mixing effects in resolving the puzzle in the dramatic increase of charge radius from ^{152}Yb to ^{154}Yb. The low-energy structure of ^{156}Yb is dominated by the quadrupole vibrational motions with a large anharmonicity, instead of shape coexistence, while ^{158}Yb is more like a prolate rotor with triaxial γ softness. Moreover, the excitation energy for the bandhead state of γ band turns out to be lowest in ^{160,162,164}Yb, depending on the details of the calculations.

ACKNOWLEDGMENTS

This work was partly supported by the Science and Technology Program of Guizhou Province (No. LH [2016] 7074), the foundation of Guizhou Minzu University (010), and the National Natural Science Foundation of China under Grants No. 11564005, No. 11765015, and No. 11575148.

[1] T. Duguet, M. Bender, P. Bonche, and P.-H. Heenen, Phys. Lett. B **559**, 201 (2003).
[2] R. R. Rodriguez-Guzman, J. L. Egido, and L. M. Robledo, Phys. Rev. C **69**, 054319 (2004).
[3] M. Bender, P. Bonche, T. Duguet, and P.-H. Heenen, Phys. Rev. C **69**, 064303 (2004).
[4] K. Nomura, T. Otsuka, R. R. Rodriguez-Guzman, L. M. Robledo, and P. Sarriguren, Phys. Rev. C **84**, 054316 (2011).
[5] J. M. Yao, M. Bender, and P.-H. Heenen, Phys. Rev. C **87**, 034322 (2013).
[6] K. Nomura, R. Rodriguez-Guzman, and L. M. Robledo, Phys. Rev. C **87**, 064313 (2013).
[7] P. Sarriguren, R. Rodriguez-Guzman, and L. M. Robledo, Phys. Rev. C **77**, 064322 (2008).
[8] G. D. Sprouse, J. Das, T. Lauritsen, J. Schecker, A. Berger, J. Billowes, C. H. Holbrow, H. E. Mahnke, and S. L. Rolston, Phys. Rev. Lett. **63**, 1463 (1989).
[9] A. E. Barzakh, I. V. Chubukov, D. V. Fedorov, V. N. Panteleev, M. D. Seliverstov, and Y. M. Volkov, Phys. Rev. C **61**, 034304 (2000).
[10] C. Xu, H. Hua, X. Q. Li, J. Meng, Z. H. Li, F. R. Xu, Y. Shi, H. L. Liu, S. Q. Zhang, Z. Y. Li *et al.*, Phys. Rev. C **83**, 014318 (2011).
[11] A. Valor, P. H. Heenen, and P. Bonche, Nucl. Phys. A **671**, 145 (2000).
[12] R. Rodríguez-Guzmán, J. L. Egido, and L. M. Robledo, Nucl. Phys. A **709**, 201 (2002).
[13] T. Nikšić, D. Vretenar, and P. Ring, Phys. Rev. C **73**, 034308 (2006); **74**, 064309 (2006).
[14] M. Bender and P.-H. Heenen, Phys. Rev. C **78**, 024309 (2008).
[15] J. M. Yao, J. Meng, P. Ring, and D. Pena Arteaga, Phys. Rev. C **79**, 044312 (2009).
[16] J. M. Yao, J. Meng, P. Ring, and D. Vretenar, Phys. Rev. C **81**, 044311 (2010).
[17] T. R. Rodríguez and J. L. Egido, Phys. Rev. C **81**, 064323 (2010).
[18] J. M. Yao, H. Mei, H. Chen, J. Meng, P. Ring, and D. Vretenar, Phys. Rev. C **83**, 014308 (2011).
[19] J. M. Yao, J. Meng, P. Ring, Z. X. Li, Z. P. Li, and K. Hagino, Phys. Rev. C **84**, 024306 (2011).
[20] T. R. Rodríguez and J. L. Egido, Phys. Rev. C **84**, 051307 (2011).
[21] T. R. Rodríguez and J. L. Egido, Phys. Lett. B **705**, 255 (2011).
[22] J. M. Yao, K. Hagino, Z. P. Li, J. Meng, and P. Ring, Phys. Rev. C **89**, 054306 (2014).
[23] T. R. Rodriguez, Phys. Rev. C **90**, 034306 (2014).
[24] J. Libert, M. Girod, and J.-P. Delaroche, Phys. Rev. C **60**, 054301 (1999).
[25] L. Próchniak, P. Quentin, D. Samsoen, and J. Libert, Nucl. Phys. A **730**, 59 (2004).
[26] T. Nikšić, Z. P. Li, D. Vretenar, L. Prochniak, J. Meng, and P. Ring, Phys. Rev. C **79**, 034303 (2009).
[27] Z. P. Li, T. Nikšić, D. Vretenar, J. Meng, G. A. Lalazissis, and P. Ring, Phys. Rev. C **79**, 054301 (2009).
[28] T. Nikšić, D. Vretenar, and P. Ring, Prog. Part. Nucl. Phys. **66**, 519 (2011).

[29] H. Mei, J. Xiang, J. M. Yao, Z. P. Li, and J. Meng, Phys. Rev. C **85**, 034321 (2012).
[30] J. M. Yao, Z. P. Li, K. Hagino *et al.*, Nucl. Phys. A **868-869**, 12 (2011).
[31] Y. Fu, H. Mei, J. Xiang, Z. P. Li, J. M. Yao, and J. Meng, Phys. Rev. C **87**, 054305 (2013).
[32] J. Xiang, J. M. Yao, Y. Fu, Z. H. Wang, Z. P. Li, and W. H. Long, Phys. Rev. C **93**, 054324 (2016).
[33] J.-P. Delaroche, M. Girod, J. Libert, H. Goutte, S. Hilaire, S. Peru, N. Pillet, and G. F. Bertsch, Phys. Rev. C **81**, 014303 (2010).
[34] P. Ring and P. Schuck, *The Nuclear Many-Body Problem* (Springer-Verlag, Berlin, 1980).
[35] Z. P. Li, T. Niksic, P. Ring, D. Vretenar, J. M. Yao, and J. Meng, Phys. Rev. C **86**, 034334 (2012).
[36] N. Hinohara, Z. P. Li, T. Nakatsukasa, T. Niksic, and D. Vretenar, Phys. Rev. C **85**, 024323 (2012).
[37] M. Girod and B. Grammaticos, Nucl. Phys. A **330**, 40 (1979).
[38] P. W. Zhao, Z. P. Li, J. M. Yao, and J. Meng, Phys. Rev. C **82**, 054319 (2010).
[39] Y. Tian, Z. Y. Ma, and P. Ring, Phys. Lett. B **676**, 44 (2009).
[40] E. Chabanat, P. Bonche, P. Haensel, J. Meyer, and F. Schaeffer, Nucl. Phys. A **635**, 231 (1998).
[41] P. Bonche, H. Flocard, and P.-H. Heenen, Comput. Phys. Commun. **171**, 49 (2005).
[42] L. Próchniak, K. Zając, K. Pomorski, S. G. Rohoziński, and J. Srebrny, Nucl. Phys. A **648**, 181 (1999).
[43] National Nuclear Data Center, Brookhaven National Laboratory, http://www.nndc.bnl.gov/index.jsp.
[44] K. Heyde and R. A. Meyer, Phys. Rev. C **37**, 2170 (1988).
[45] I. Angeli, At. Data Nucl. Data Tables **87**, 185 (2004).
[46] S. Quan, W. P. Liu, Z. P. Li, and M. S. Smith, Phys. Rev. C **96**, 054309 (2017).
[47] K. Hagino and J. M. Yao, Phys. Rev. C **91**, 064606 (2015).
[48] J. M. Yao, E. F. Zhou, and Z. P. Li, Phys. Rev. C **92**, 041304 (2015).